

TECHNICAL REPORT

Contract Title: Infrared Algorithm Development for Ocean Observations
with EOS/MODIS
Contract: NAS5-31361
Type of Report: Semi-Annual
Time Period: January- June 1999
Principal Investigator: Otis B. Brown
RSMAS/MPO
University of Miami
4600 Rickenbacker Causeway
Miami, Florida 33149-1098

INFRARED ALGORITHM DEVELOPMENT FOR OCEAN OBSERVATIONS WITH EOS/MODIS

Abstract

Efforts continue under this contract to develop algorithms for the computation of sea surface temperature (SST) from MODIS infrared measurements. These include radiative transfer modeling, comparison of *in situ* and satellite observations, development and evaluation of processing and networking methodologies for algorithm computation and data access, evaluation of surface validation approaches for IR radiances, development of experimental instrumentation, and participation in MODIS (project) related activities. Activities in this contract period have focused on field campaigns, analysis of field data and the organization of and participation in two workshops held at RSMAS in early March.

MODIS INFRARED ALGORITHM DEVELOPMENT

A. Near Term Objectives

- A.1. Continue algorithmic development efforts based on experimental match-up databases and radiative transfer models.
- A.2. Continue interaction with the MODIS Instrument Team through meetings and electronic communications, and provide support for MCST pre-launch calibration activities.
- A.3. Continue evaluation of different approaches for global SST data assimilation and work on statistically based objective analysis approaches.
- A.4. Continue evaluation of high-speed network interconnection technologies.
- A.5. Continue development of *in situ* validation approaches for the MODIS IR bands.
- A.6. Provide investigator and staff support for the preceding items.

B. Overview of Current Progress

B.1 January – June 1999

Activities during the past six months have continued on the previously initiated tasks. There have been specific efforts in the areas of (a) IR calibration/validation as part of the MODIS Ocean Science Team cruise effort; (b) a theoretical assessment of the MODIS instrument errors on the retrieval of SST; and (c) testing and evaluation of an experimental wide area network based on ATM technology. In addition, previously initiated activities, such as team related activities, continue.

Special foci during this six-month period have been:

- 1) Refinement of the radiative transfer model used to simulate the MODIS infrared measurements and the derivation of the atmospheric correction algorithm for SST retrieval.
- 2) Continuation of the development and refinement of the at-launch sea-surface temperature retrieval algorithms
- 3) MODIS-PFM and FM-1 IR pre-launch characterization interactions.
- 4) Continuation of the analysis of measurements from M-AERI research cruises (Table 1).
- 5) Preparation and participation in the cruise of the USCGC Polar Sea from Australia to Seattle, via the St. Lawrence Island Polynya in the Bering Strait (March to May 1999).
- 6) Preparation and participation in the cruise of the R/V Mirai in the Tropical Pacific Ocean, as part of the Nauru99 Campaign (June - July 1999).
- 7) A visit to the Institute of Atmospheric Physics, University of Rome, to discuss collaborative field experiments on the effects of aerosols on the retrievals of SST from space-borne infrared radiometry.
- 8) A visit to the Alfred-Wegener Institute of Polar and Marine Research, Bremerhaven, Germany, to conclude discussions on using a M-AERI during a cruise of the PFS Polarstern,
- 9) Continuation of negotiations for ship-time for post-launch validation, and exploration of options for long-term validation from fixed platforms.
- 10) Development of a purpose-built computer data-base for validation cruise data and

associated satellite measurements.

- 11) Implementation of various SST data assimilation approaches.
- 12) Refinement of marine FTIR instrumentation and software (including Y2K compliance) for cal/val applications by UW-SSEC through a subcontract.
- 13) Establish a collaboration with Dr B. Ward of the Nansen Environmental and Remote Sensing Centre, Bergen, Norway, to study the thermal skin layer with his micro-profiler and the M-AERI.
- 14) Specify and purchase a high-stability, high-accuracy water-bath, black-body, calibration target for the M-AERIs from Hart Scientific Inc. with guidance from NIST personnel.
- 15) Enhancement of wide-area networking.

B.1.1 Refinement of the radiative transfer model

Dr Albin Závody spent six weeks at RSMAS in February-March 1999. He is the author of the forerunner of the radiative transfer model used in the simulations of the MODIS infrared measurements, which has been used for simulations of AVHRR and ATSR. During his visit he worked closely with Drs Richard Sikorski and Peter Minnett on refining the MODIS simulation model.

B.1.1.1. Spectral parameters.

The model was updated with improved spectra for atmospheric components from the AFGL data base. Coverage of the model was extended to include the 8.6 μ m range for MODIS band 29. The model now covers the spectral ranges of 3.5 to 4.2 μ m and 6.2 to 14.7 μ m.

B.1.1.2. Band averaged emissivities

Refined band averaged emissivities were computed for each of the MODIS bands (and for AVHRR instruments on NOAA-7 to NOAA-14). Selection of the instrument band at the beginning of the program automatically identifies the emissivity appropriate for the frequency response used in the brightness temperature calculations.

B.1.1.3. Aerosol effects.

The model was modified to include additional options for winter and summer desert-type tropospheric aerosols, as described in d'Almeida, et al. (d'Almeida G, Koepke, P, & Shettle, E P: Atmospheric Aerosols, Deepak Co, 1991). The input parameters are the type of aerosol (summer type or winter type), the aerosol optical depth, and the lower and upper boundaries of the aerosol layer (in height). The aerosol concentration is assumed to vary as sine-square with height, and equal to zero at the boundaries. A start was made in investigating whether the increase in brightness temperature deficits can be determined if additional desert type aerosols are present in the field of view, with the optical depth at 0.55 μ m also known. The results for

MODIS bands 31 and 32 are shown in Figure 1 for desert type aerosols of the summer and winter type. The figures show that effect on brightness temperatures is close to linear with optical depth at $0.55\mu\text{m}$, but also that the strength of the effect depends strongly on both the height of the aerosol layer, and whether the aerosols are of summer or winter type. The absence of a spectral signature between the two channels implies that the chances of a simple correction are not great.

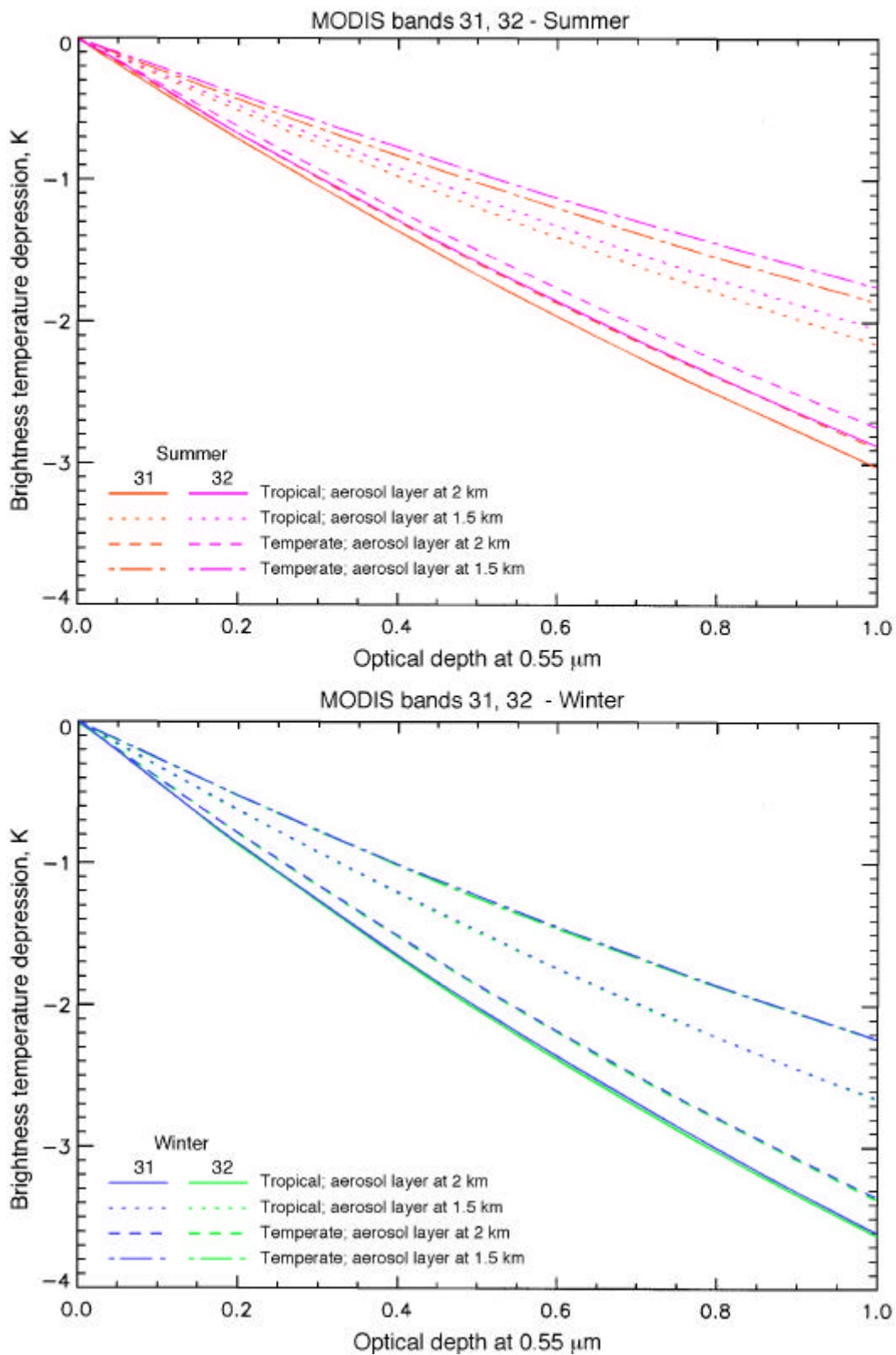


Figure 1. Simulations of the effects of tropospheric aerosols on the MODIS brightness temperatures in Bands 31 and 32. The lack of a spectral signature is apparent.

B.1.1.4. Atmospheric characterization

A data base consisting of 2790 atmospheric profiles based on the output from the ECMWF assimilation model was installed at RSMAS. These are from 1996 and provide good global oceanic coverage at 10° latitude-longitude nodes, good seasonal distribution, and some day/night content (noon and midnight UTC for the 1st of every other month). The distributions are shown in Figure 2. Gaps in the distributions are where clouds are presumed present by high relative humidity values ($>95\%$ at any level in the profile).

B.1.1.5. Ozone profile

There is strong ozone absorption at $9.5\mu\text{m}$ but ozone absorption lines are also present both at shorter and longer wavelengths. The model takes into account ozone absorption but the same ozone profile is used in all the brightness temperature calculations. The effect of ozone was checked by taking the differences in brightness temperatures calculated with and without ozone. The largest differences for the nadir view, using the tropical, mid-latitude and high-latitude US standard atmospheric profiles, are given in Table 1.

Table 1. The maximum effects of ozone on MODIS band brightness temperatures.

MODIS Band	Difference
29	310 mK
31	1 mK
32	13 mK

The ozone profile used was that for the mid-latitude summer where the column ozone was 6.95 g m^{-2} . For the tropical profile the amount is 22% lower, and for the high latitude profile 24% higher. Hence, roughly, the ozone effects in Band 32 would be approximately $0.78 \times 13 \text{ mK}$ and $1.24 \times 13 \text{ mK}$ for the tropics and high-latitudes, i.e. in error by $0.22 \times 13 \text{ mK}$ ($= 3 \text{ mK}$) and $-0.24 \times 13 \text{ mK}$ ($= -3 \text{ mK}$). Compared to other uncertainties, due to aerosols *etc*, these errors are not significant for MODIS bands 31 and 32, and there is no need to use latitudinally more representative ozone concentrations in the simulations. The ozone effect is much stronger in MODIS band 29: variation in ozone concentrations can change the brightness temperatures by 60 mK or more, even in the nadir view. Hence it may be necessary to make the ozone profile an additional input parameter in the simulations for this band.

B.1.1.6. Polarization sensitivity.

For angles different from the local vertical to the sea surface, the radiation emitted is always polarized to some extent as the surface emissivities are different for horizontal and vertical polarization. If the instrument measuring the upwelling radiation is polarization sensitive then the output signal is not uniquely determined by the photon flux intercepted. Table 2 shows results for viewing the sea surface at an across-track distance of 1000 km. The emissivity ratios for the two polarizations are given in the second column, and the differences in the simulated brightness temperatures for the two polarizations in column 3 to 5, for the three standard US atmospheres. The last three columns give the ratio of the photon fluxes.

ECMWF Profile Distributions for R.S.M.A.S. ThIR Modeling

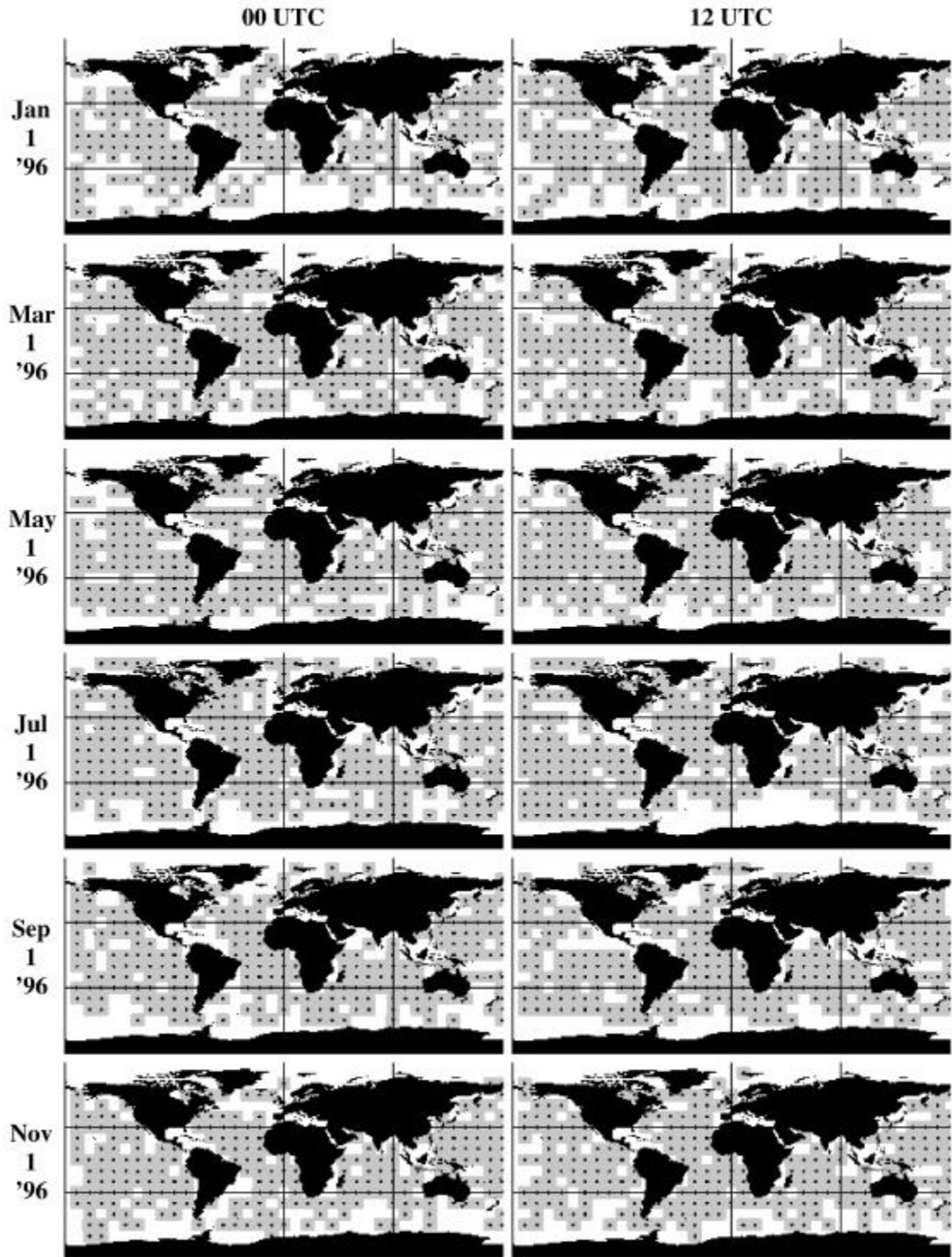


Fig 2. Distribution of atmospheric profiles derived from the ECMWF assimilation model.

Table 2. Polarization effects on the MODIS infrared bands to be used for SST determination. For a pixel at 1000km from the sub-satellite point.

MODIS Band	Emis-sivity ratio	Brightness temperature difference			Ratio of photon fluxes		
		Tropical	Mid-latitude	High-latitude	Tropical	Mid-latitude	High-latitude
20	0.875	2.114	2.157	2.178	0.913	0.908	0.893
22	0.882	2.320	2.257	1.962	0.908	0.907	0.882
23	0.883	1.608	1.514	1.270	0.935	0.937	0.938
29	0.907	1.272	1.973	3.200	0.975	0.961	0.928
31	0.945	0.207	0.660	2.413	0.997	0.990	0.957
32	0.907	0.271	0.995	4.225	0.996	0.986	0.931

For the shorter wavelength bands the emissivities are slightly lower, hence the emissivity ratios are smaller. Atmospheric water vapor, however, affects the bands less and therefore the brightness temperature differences are very similar for the three atmospheric profiles. The opposite is true for the longer wavelength bands: the tropical atmosphere is the most absorbing of the three and hence contributes most of the unpolarized radiation, consequently the brightness temperature differences are the smallest in this case. No figures are currently available for the polarization sensitivity of MODIS, hence the value (0.97) for the ATSR-2 3.7 μ m channel was used. In this case, the worst case error was 4 mK. Hence, provided MODIS's polarization sensitivity is not significantly worse than 0.97, the effect can be ignored. (N.B. error here means the difference between brightness temperatures derived from the same photon flux, in one case polarized, in the other unpolarized.)

B.1.1.7. *Photon-counter vs power radiometer.*

The channel relative response functions of infrared radiometers are not always true ratios, as the background is often measured by a power detector, whereas the radiometer, in most cases, measures photon counts. The model can generate brightness temperature spectra for either case, by setting the 'photon' parameter to 0 or 1. In the MODIS case the effect of using different types (photon/power) detectors for deriving the frequency response was investigated by using three representative atmospheric profiles. For bands in the 4 μ m window, the effect was found to be less than 0.01K. It was also only marginally significant for band 32, with a maximum value of 0.03K. (N.B. The figures are for the nadir view, for an oblique view with 1.75 air masses the values are about 20% higher.)

B.1.7. At-launch algorithms

With these modifications, we conducted further regressions for evaluation of MODIS SST algorithms and delivery of pre-launch coefficients for the 11-12 μ m and the 3-4 μ m bands.

B.1.7.1. *11-12 μ m algorithm*

For the 11-12 μ m algorithm, we confirmed that the relationship between channel difference and

SST changes at around 0.7 K, which is how the current algorithm is implemented. Residuals increase and the relationship of SST to brightness temperature changes considerably at satellite zenith angles greater than 30°. Other factors studied included the optical thickness of tropospheric aerosols, and polarization effects in the MODIS thermal infrared bands (see above). In addition, comparisons were run of direct ship-board interferometer SST measurements (M-AERI), AVHRR 11-12µm brightness temperatures, and our RAL-modeled brightness temperatures for those channels. This study supports the utility of our radiative transfer modeling for MODIS SST algorithm development and generation of pre-launch coefficients.

B.1.7.2. 3.5-4.2µm algorithm

The simulations to derive the 3.5-4.2µm atmospheric correction algorithm were done before the new data base of ECMWF atmospheric profiles was installed, and so the results presented here are based on the atmospheric profiles from a globally distributed set of 761 quality-controlled coastal and marine radiosondes (Figure 3). Since the radiosondes do not include coincident SSTs, SST is taken to range from 0.5 K colder than the surface air temperature to 1.5 K warmer, in half-degree steps. The radiosondes profiles are also be used as sources for correlative data: date and time, location, total vapor, and structure of the atmospheric temperature and water vapor profile. As with the simulations of band 31 and 32 (see earlier reports), the satellite zenith angles were selected as fractions from one to two atmospheric path-lengths, at 10° increments from vertical, for a total of 9 possible zenith angles (one atmosphere path-length = vertical viewing angle).

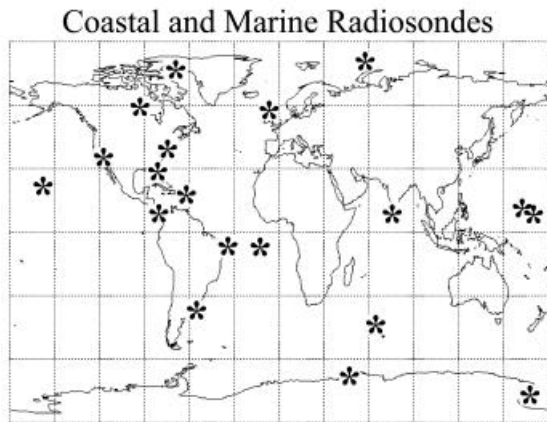


Figure 3. Distribution of coastal and marine radiosonde stations providing data used in the simulations.

Brightness temperatures at the top of the atmosphere were calculated for MODIS bands 20, 22, and 23. These were used with the SSTs to generate sets of coefficients using a robust regression technique. Initially, we structured the algorithm as a simple multi-channel SST (MCSST) expression for band pairs 20 and 22, 20 and 23, and 22 and 23:

$$SST = a * T_a + b * T_b + c$$

where T_a is the brightness temperature at the shorter-wavelength band of each pair, and T_b is at the longer-wavelength band; a , b , and c are coefficients. The algorithm-generated SSTs are fairly well spread over the range of SSTs (Figure 4).

When stratospheric aerosols are elevated to 50-times normal background levels, however, a bi-modal distribution can be seen in residuals versus reference SSTs, especially in the 20 and 22 (Figure 5), and 22 and 23 band pairs. This bi-modal distribution could not be resolved versus total atmospheric vapor (Figure 6), channel difference, surface temperature difference from mean radiosonde temperature, water vapor scale height, or versus the difference of the sea surface temperature from the mean temperature below the vapor scale height. This property of

the data (with elevated stratospheric aerosols) did appear strongest at low latitudes, and the relationship of residuals to solar zenith angle varied with latitude (Figure 7).

A seasonal term was added to each algorithm, using noon solar zenith angle as the parameter:

$$SST = a * T_a + b * T_b + c + m * \cos(2\pi * (x + n) / 365) + p$$

where:

m , n , and p are coefficients

x (northern hemisphere)=days after 173 (summer solstice)

x (southern hemisphere)=days after 357 (winter solstice)

for leap years, standard year days = leap year days * 365/366

This was further resolved with latitude-specific coefficients. Under normal stratospheric aerosol loads, the seasonal component is very weak, and is not a significant factor in limiting accuracy. Table 3 gives the coefficients and rms uncertainties for the 20 and 22 band pair (for temperatures in Celcius degrees). The rms uncertainties are small, and the improvement in going to more complex algorithms marginal. For elevated stratospheric aerosol cases, the rms uncertainties improved by one-third or better, but even so are at the 0.33K level at best.

Table 3. Algorithm characteristics for the Bands 20 and 22 simulations.

Latitude (λ) range	Coefficients						rms K
	a	b	c	m	n	p	
All λ	1.64127	0.00800621	1.01518	0.0	0.0	0.0	0.171
Include seasonal effects:							
All λ	1.64127	0.00800621	1.01518	-0.021444	-28.43	-0.010729	0.172
Include seasonal and latitudinal effects:							
$ \lambda < 23.45$	1.64127	0.00800621	1.01518	-0.021115	-65.39	+0.018334	0.163
$23.45 \geq \lambda \geq 46.9$	1.64127	0.00800621	1.01518	+0.023730	-59.5	-0.092053	
$ \lambda > 46.9$	1.64127	0.00800621	1.01518	-0.021444	-28.43	-0.010729	

There is a strong correlation between total water vapor and the Band 20-22 and Band 20-23 differences. Some evidence was found of breakpoints at about 0.1 and 1.0K in each of these band-pair brightness temperature differences, similar to the breakpoint at 0.7 K used in the bands 31 and 32 algorithm, but for these bands the location of the inflections appears to be dependent on viewing angle over a broad range. As with the band 31 and 32 simulations, residuals are smaller when the viewing angle is less than 30 degrees, although the viewing angle dependence is still being investigated.

B.1.3 MODIS-PFM and FM-1 IR Pre-launch Characterization

Drs. Otis Brown and Peter Minnett provided input to the Project and Program management

concerning pre-launch characterization issues associated with the MODIS PFM and FM-1 instruments.

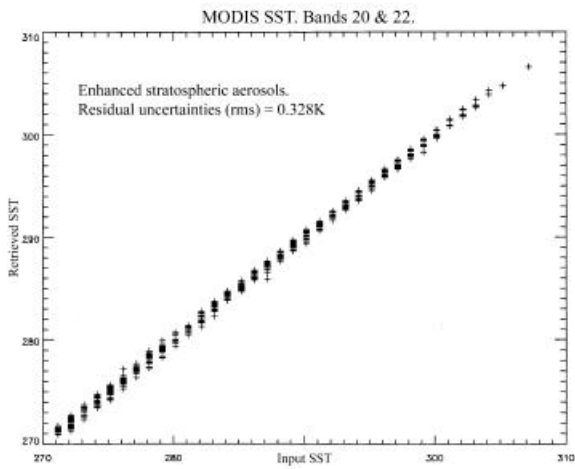


Figure 4. Simulated SST retrievals from MODIS Bands 20 and 21.

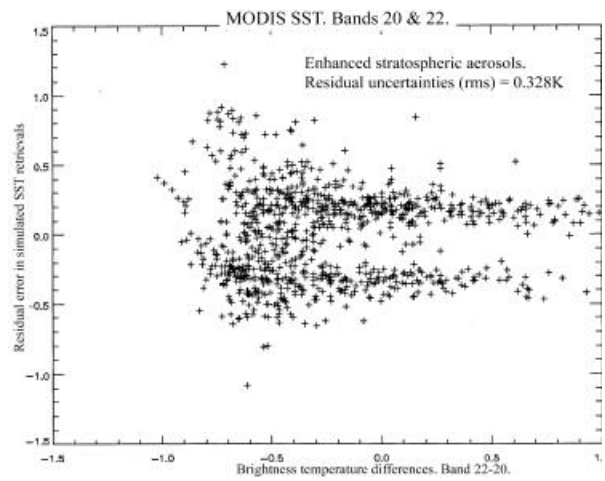


Figure 5. Simulated residual error in SST as a function of difference in the Bands 20 and 22 brightness temperatures.

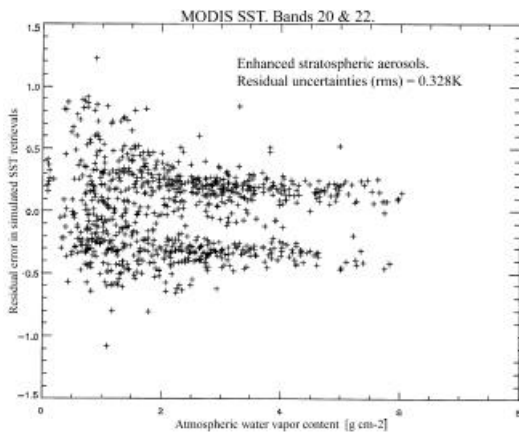


Figure 6. Simulated residual error in SST as a function of atmospheric water vapor content.

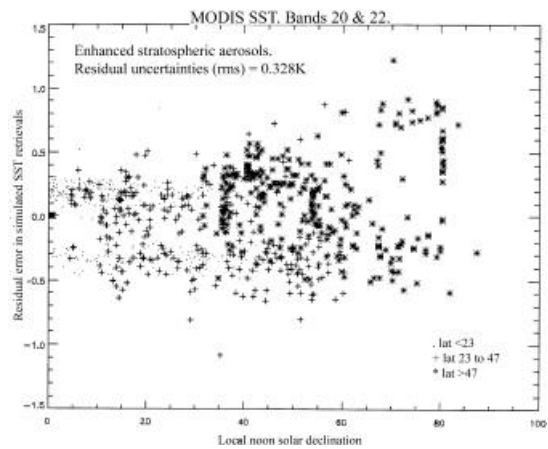


Figure 7. Simulated residual error in SST as a function of solar declination at local noon. The points are stratified by the modulus of latitude.

B.1.4. Completed M-AERI cruises.

The M-AERI research cruises (Figure 8; Table 4) in a wide range of climatic regimes have produced a unique data set for the study of the oceanic thermal skin layer and its response to surface forcing. The latest two cruises in Table 4 are discussed in this report; earlier cruises have been discussed in prior reports. The knowledge gained from analysis of these data sets will be important to improved understanding the results of the post-launch MODIS SST validation measurements. In addition to the continuing scientific analyses of these data, work has begun on constructing a database for the archiving and retrieval of the cruise data. While the M-AERI measurements are a consistent data set, the ancillary measurements (surface meteorology, radiosondes etc.) are less so, depending on the instrumentation already installed on the ship or installed by other cruise participants. Importing these diverse data sets into a uniform database will aid efficient data access and analysis in the MODIS post-launch period (see section B.1.10 below)

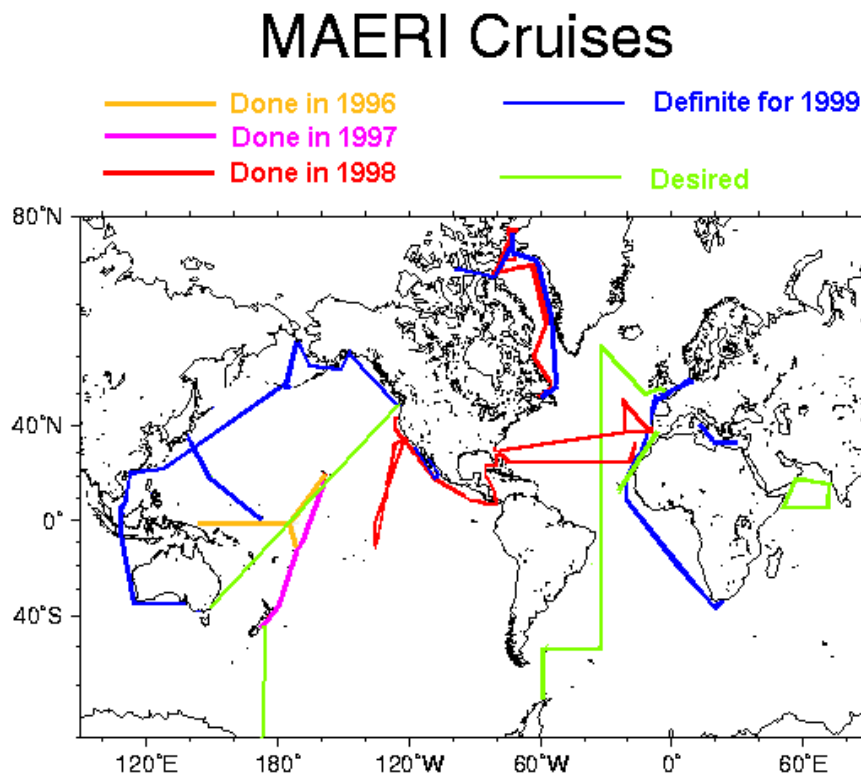


Figure 8. Schematic cruise tracks of M-AERI deployments. The 1999 cruises completed in this period are the USCGC *Polar Sea* (blue track from Australia to Seattle) and the R/V *Mirai* (blue track to/from Japan to the Equator).

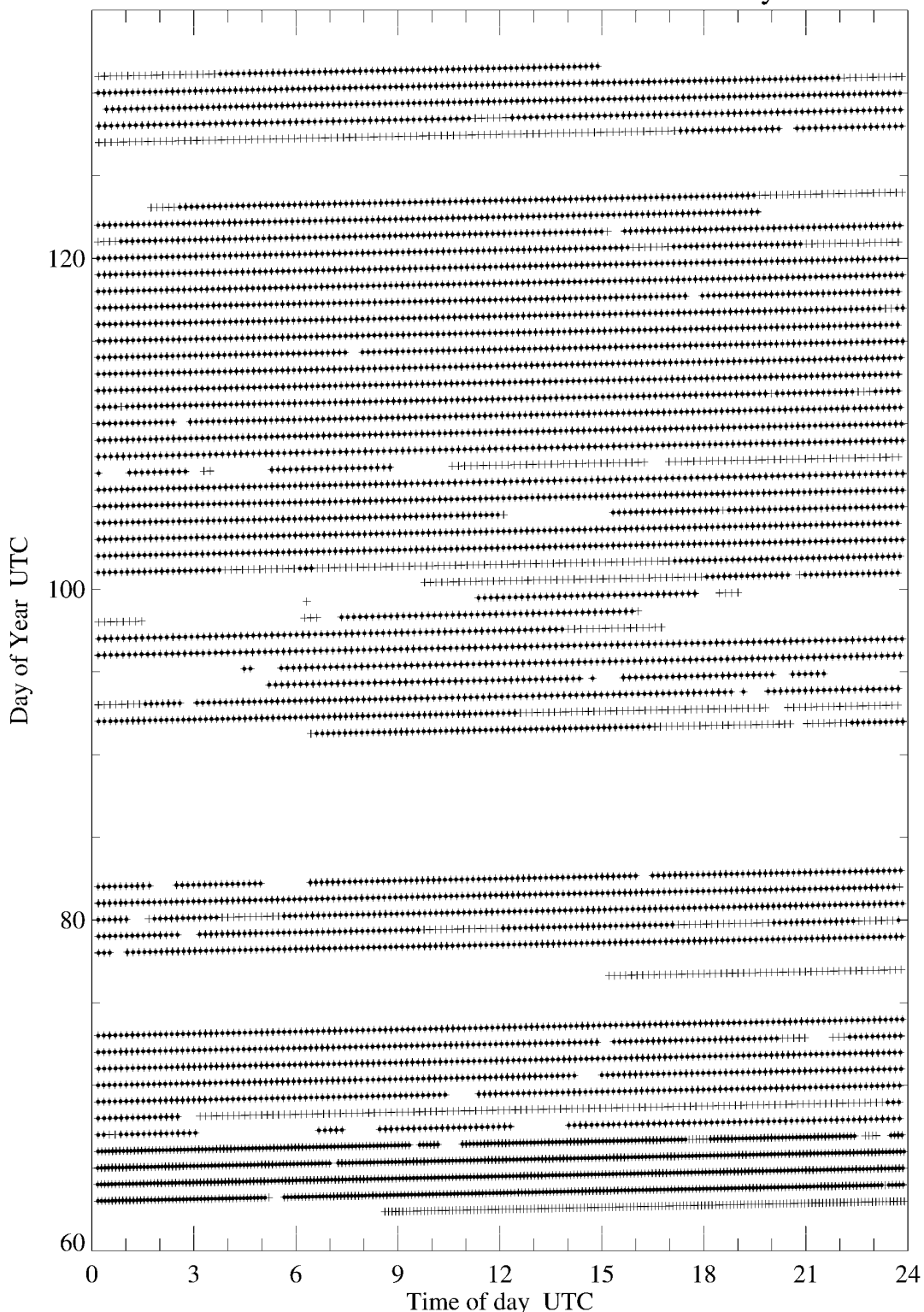
Table 4. Completed M-AERI cruises

Project	Ship	Dates	Ports
Proof of concept	R/V Pelican	15-17 Jan 95	LUMCON, LA
Combined Sensor Cruise	NOAA S Discoverer	14 Mar – 13 Apr 96	Pago-pago, American Samoa. Honolulu, HI
Hawaii – New Zealand Transect	R/V Roger Revelle	28 Sept - 14 Oct 97	Honolulu, HI. Lyttleton, NZ
OACES 24 N Section	NOAA S Ronald H. Brown	8 Jan. - 24 Feb 98	Miami, FL. Las Palmas, Canary Islands, Spain. Miami, FL
NOW 98	CCGS Pierre Radisson	26 Mar - 28 Jul 98	Quebec City, Canada. Nanisivic, Canada
OACES Gasex-98	NOAA S Ronald H. Brown	2 May - 7 Jul 98	Miami, FL. Lisbon & Ponta Delgada, Portugal. Miami, FL
Panama Transit	NOAA S Ronald H. Brown	12-27 Jul 98	Miami, FL. Newport, OR
PACS-Mooring recovery	R/V Melville	8-29 Sept 98	San Diego, CA
Pacific Transect and SLIP99	USCGC Polar Sea	5 March – 12 May 99	Adelaide, Australia. Perth, Australia. Benoa, Indonesia. Hong Kong, China. Dutch Harbor AK. Anchorage, AK. Seattle, WA.
Nauru99	R/V Mirai	8 June -10 July 99	Yokohama, Japan. Sikenehama, Japan.

B.1.5 The Pacific Transect and SLIP99 cruise of the USCGC *Polar Sea*

Each year the USCGC *Polar Sea*, or its sister ship the USCGC *Polar Star*, travels from its home port of Seattle to resupply the US Antarctic bases, leaving in November and returning in March-April. The voyage passes through a wide range of climatic regimes and is therefore an attractive opportunity to validate the atmospheric correction algorithms used to derive SST from MODIS, or AVHRR in the pre-launch period. The return cruise of the *Polar Sea* in early 1999 was extended to include a three-week research cruise to the St. Lawrence Island Polynya in the Bering Strait (SLIP99), so the cruise was both longer and covered an extended range of latitudes. A team from RSMAS traveled on the *Polar Sea* from Australia to Seattle to make measurements using the M-AERI and ancillary

USCGC Polar Sea. MAERI-2. 5 March - 11 May 1999



Peter J. Minnett, RSMAS-MPO. Fri Sep 10 16:24:49 1999 e:\PolarSea99\mltps99_MAERI_data.ps

Figure 9. Data return from the M-AERI. Each cross represents an independently calibrated set of spectra, including those taken when the instrument was covered to protect against spray. Dots are high-quality data taken of the ocean or ice surface and atmosphere, from which skin temperatures have been derived. Gaps are when the system was down. Day 80 is March 21, and day 130 is May 10.

equipment throughout the cruise as a test of the suitability of the *Polar Sea* as a platform for MODIS validation. The M-AERI was mounted above the wheelhouse, looking over the port side ahead of the bow wave, and a weather station mounted ahead of the wheelhouse. An all-sky camera was installed above the helicopter hangar and radiosondes were launched from the helicopter deck.

The ship sailed from Port Adelaide, South Australia, March 5 (23:30, March 4, UTC) and headed to Dutch Harbor in Alaska via Fremantle in Western Australia, Benoa in Indonesia, and Hong Kong. The scientific complement for the SLIP99 cruise joined in Dutch Harbor, and the *Polar Sea* headed towards St Lawrence Island in the Bering Strait for about 14 days of biological research. The ship returned to Seattle, arriving on May 12 after a brief port call in Anchorage. The schematic cruise track is apparent in Fig 8 and the M-AERI data return is shown in Figure 9

B.1.6. The Nauru99 cruise of the *R/V Mirai*.¹

The cruise of the *R/V Mirai* in June-July 1999 was part of the international Nauru99 campaign, which involved the NOAA S Ronald H. Brown and the DOE ARM (Atmospheric Radiation Measurements program) ARCS (Atmospheric Radiation and Cloud Station) on the island of Nauru (0.5°S, 166.9°E). The Nauru99 campaign was designed to take measurements with which to address several hypotheses relating the influence of convective clouds, that are generated by small islands, on the surface radiation budget. For the objectives of this project, the *R/V Mirai* provided a very good platform for the validation of sea-surface temperatures derived from satellite-borne infrared radiometers. The track of the ship (Figure 10) passed through the several distinct atmospheric regimes including down-wind of the Japanese mainland, where the tropospheric aerosol burden is high; the northern trade wind zone; and the Inter-Tropical Convergence Zone (ITCZ) where atmospheric water vapor burdens are very high and the troposphere very deep. The ITCZ especially presents particularly difficult conditions for infrared SST measurements from space.

The *R/V Mirai* sailed from Yokohama on 8 June and headed towards Nauru, calling in at Chuuk en route (Figure 10). From June 17 to July 4 the *Mirai* was in the close vicinity of Nauru. On the return journey, most of the scientific equipment and scientific crew left the ship in Majuro, but the M-AERI and several other projects remained on board to continue measurements on the section to Japan. Unfortunately the M-AERI measurements were brought to a close following an accident on July 9 in which Jennifer Hanafin, a graduate student at RSMAS who was on board to operate the M-AERI, fell and broke her leg. The ship diverted to Guam, where Jennifer was admitted to the Guam Memorial Hospital where she had surgery. She is now recovering at her home in Ireland.

The M-AERI was mounted on a foremast platform with a clear view ahead of the bow-wave of the ship. The instrument was run continuously and initial inspection indicates that the data are of good quality and rate of return is high. The surface float carrying a precision thermistor was deployed when the ship was on station and was used to measure the bulk surface temperature at a depth of a

¹ Funding for the *R/V Mirai* cruise was provided through a separate grant to P.J. Minnett, but it is included here for the sake of completeness of discussion of the M-AERI cruises.

few centimeters with an accuracy $\sim 0.01K$. Ancillary measurements were taken by instruments belonging to other US and Japanese groups on board. For example, 179 radiosondes were launched during the

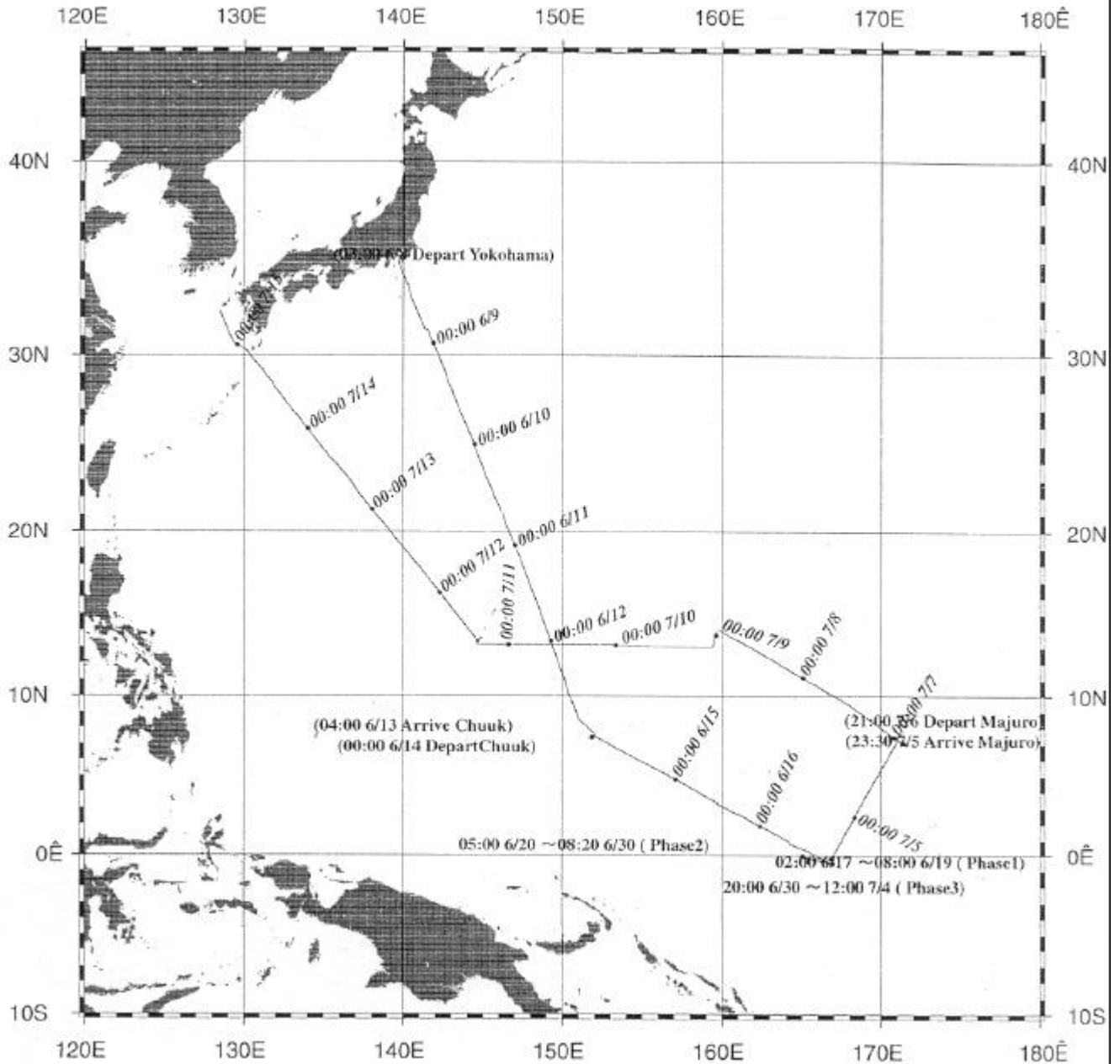


Figure 10. Cruise track of the R/V Mirai during the Nauru99 campaign. (Figure taken from the Cruise Report, published by JAMSTEC, Yokosuko, Japan).

B.1.7. Collaboration with the Institute of Atmospheric Physics, Italy².

Discussions have begun with Drs R. Santolieri, E. Böhm, and others at the Institute of Atmospheric Physics (IFA), Rome, Italy, on possible future collaborative studies on the influence of aerosols on satellite remote sensing. Dr. Peter Minnett visited IFA in June and gave a seminar. He also finalized plans for a collaborative research cruise in October-November 1999 on the Italian ship *R/V Urania*. Two RSMAS scientists and equipment will participate in the cruise.

B.1.8. Collaboration with the Alfred Wegener Institute for Polar and Marine Research, Germany².

While in Germany to attend the IGARSS Symposium in Hamburg, Dr. Peter Minnett spent a day at the Alfred Wegener Institute for Polar and Marine Research in Bremerhaven to conclude discussions on the use of the PFS *Polarstern* as a suitable platform for MODIS validation. The *Polarstern* is a well equipped ice-breaking research vessel that travels to and from Antarctica each year, thus passing through a wide range of atmospheric conditions, including the aerosol regime off West Africa. Dr Minnett met with Prof. Augstein and Drs Fahrbach and König-Langeloe. Space and resources will be made available on the ship for two scientists and instrumentation for the passage from Bremerhaven to Cape Town during December 1999 and January 2000.

B.1.9. Validation cruises

As a result of the delay in the launch of the EOS AM-1 platform several cruises which were planned for post-launch MODIS validation will now take place before MODIS becomes operational in orbit.

Currently planned pre-launch M-AERI cruises are:

- a) CCGS *Pierre Radisson* in the Canadian Arctic, August-October 1999.
- b) *R/V Melville* off Baja California, October 1999.
- c) *R/V Urania* off Sicily, October 1999.
- d) PFS *Polarstern*, Germany to South Africa, December 1999 – January 2000.

Post-launch M-AERI cruises which are being negotiated include:

- e) USCGC *Polar Sea* March-April 2000. Pacific Ocean, from Australia or New Zealand to Seattle.
- f) *R/V Urania* off Sardinia, March 2000.
- g) A joint US-Indian-Omani Expedition to the Arabian Sea in 2000
- h) A joint cruise with the MODIS Ocean Color Group.

² Travel funds for Dr. Minnett's visit were not provided through this contract.

Participation in some of these cruises will be contingent on securing an appropriate level of funding.

Web pages show tables with the cruises for 1999
(<http://www.rsmas.miami.edu/ir/MAERI99.html>) and earlier deployments
(<http://www.rsmas.miami.edu/ir/MAERI95-98.html>)

B.1.10. The M-AERI Data Base

Work has been progressing on the M-AERI Database that will store M-AERI data and ancillary measurements. Its purpose is to provide a convenient user interface to access M-AERI and ancillary ship-based measurements and co-located satellite data. In the absence of MODIS data, AVHRR is used as the source of satellite data.

A relational model has been built using Sybase as the Database Management System (DBMS) and Transact-SQL to create tables, insert data, and query the database. Data are retrieved through a web interface written in Perl/CGI where users can easily search the database by various options.

The M-AERI Database homepage is located at <http://www.rsmas.miami.edu/ir/maeri-db>. This page is open to the public and provides general information about M-AERI, including past, current, and future projects, pictures, and information on ancillary instruments appearing in the database. To access the database search area, a username and password must be entered. Once inside this area, the user has a variety of search options available to retrieve data. There is also a interactive list of data tables where the user can find information on the field names (variables), units, data resolution, size of table, and the date when the table was last updated. As a last step in each search option, the size of the output table is displayed and the user has the option to continue to the results, or to go back and narrow the selection. The output can be displayed in table or ASCII format and can be saved as a table or view in the database for future use.

B.1.10.1 Database Structure

Each type of data has its own set of tables with a common prefix called a 'dataname'. The dataname for M-AERI sea surface temperature data is MaeriSst and the tables are separated by project, such as MaeriSst_1, MaeriSst_2, etc. Each dataname has five key fields that are used to relate the data to index tables and other data tables. Fields are also referred to as columns or variables. The five key fields are IdDay (date id), IdData (data row id), IdName (dataname id), IdProj (project id), and IdInst (instrument id). Table 5 is a sample output from a union between MaeriSst 1 and MaeriSst_2.

Table 5 'MaeriSst Data' screen of the data base GUI.

IdDay	IdData	IdName	IdProj	IdInst	AirTemp	StdAirTemp	UncAirTemp	SkinTemp	StdSkinTemp	UncSkinTemp
77	1	1	1	0	301.099	0.084	0.021	302.403	0.091	0.029
77	2	1	1	0	301.195	0.097	0.024	302.474	0.143	0.045
78	1	1	1	0	301.181	0.097	0.024	302.062	0.145	0.046
78	2	1	1	0	300.953	0.095	0.024	302.204	0.07	0.022
637	1	1	2	2	300.924	0.086	0.022	304.7	0.076	0.024
637	2	1	2	2	301.27	0.031	0.008	301.003	0.032	0.01
638	1	1	2	1	301.189	0.061	0.015	301.246	0.089	0.028
638	2	1	2	1	301.089	0.084	0.021	301.022	0.067	0.021

Table 6 IndexDaily screen of the M-AERI database GUI.

IdDay	IdData	IdName	IdProj	IdInst	YYYYMMDD	HHMMSS	Sec1981	DecHour	Lon	Lat	Flag	BasinCode
77	1	1	1	0	19960317	015124	479872295	1.857	-176.95	-6.043	-9	3
77	1	3	1	0	19960317	014448	479871899	1.747	-176.936	-6.063	-9	3
77	1	4	1	0	19960317	014448	479871899	1.747	-176.936	-6.063	-9	3
77	2	1	1	0	19960317	021027	479873438	2.174	-176.998	-5.977	-9	3
77	2	3	1	0	19960317	014732	479872063	1.792	-176.94	-6.056	-9	3
77	2	4	1	0	19960317	014732	479872063	1.792	-176.94	-6.056	-9	3
78	1	1	1	0	19960318	003730	479954261	0.625	179.443	-2.006	-9	3
78	2	1	1	0	19960318	005627	479955398	0.941	179.36	-2.005	-9	3
637	1	1	2	2	19970928	033128	528262300	3.524	-157.886	21.316	-9	2
637	2	1	2	2	19970928	034759	528263291	3.8	-157.886	21.316	-9	2
638	1	1	2	1	19970929	085341	528368033	8.895	-158.518	20.278	-9	2
638	2	1	2	1	19970929	090010	528368422	9.003	-158.53	20.259	-9	2

Table 7 'IndexData' screen of the M-AERI database GUI.

IdDay	DataName	IdProj	IdInst	YYYYMMDD	HHMMSS	Sec1981	DecHour	Lon	Lat	BasinCode
77	MaeriSst	1	0	19960317	015124	479872295	23.577	-176.95	-6.043	3
77	MaeriRadSpectraStats	1	0	19960317	014448	479871899	1.747	-176.936	-6.063	3
77	MaeriRadSpectra	1	0	19960317	014448	479871899	1.747	-176.936	-6.063	3
78	MaeriSst	1	0	19960318	003730	479954261	23.654	179.443	-2.006	3
637	MaeriSst	2	2	19970928	033128	528262300	23.61	-157.886	21.316	2
638	MaeriSst	2	1	19970929	085341	528368033	23.803	-158.518	20.278	2

Table 8. 'IndexProj' screen of the M-AERI database

IndexData, which together hold the key relations to the data tables. IndexDaily contains a record for each date and dataname in the database and IndexData contains all of the records for each data name in the database (see Table 6 and Table 7). Other sample screens are shown in Tables 8 and 9.

B.1.10.2 *Search by Ocean Basin*

The user starts this search by choosing an Ocean Basin from the image map or list (See Figure 11). A list of

Among the index tables are the two most important, IndexDaily and

Table 9. 'IndexProj' screen of the M-AERI database GUI.

IdProj	IdMinDate	IdMaxDate	IdYear	ProjectName
1	74	104	1996	csp96
2	637	653	1997	rev97
3	738	786	1998	24n98
4	816	940	1998	now98
5	853	919	1998	gase98
6	924	939	1998	panama98
7	982	1003	1998	pacs98

InstrumentName	IdInst
maeriproof	-1
maeri00	0
maeri01	1
maeri02	2
maeri03	3
tsg	4
wpac	5
rawindsonde	6

data in that region is displayed so that the user can pick which dataname to view (i.e. MaeriSst, Met, and Rsonde). The next screen lists all the dates for that dataname from which the user can opt to view all of the dates, one date, or multiple dates.

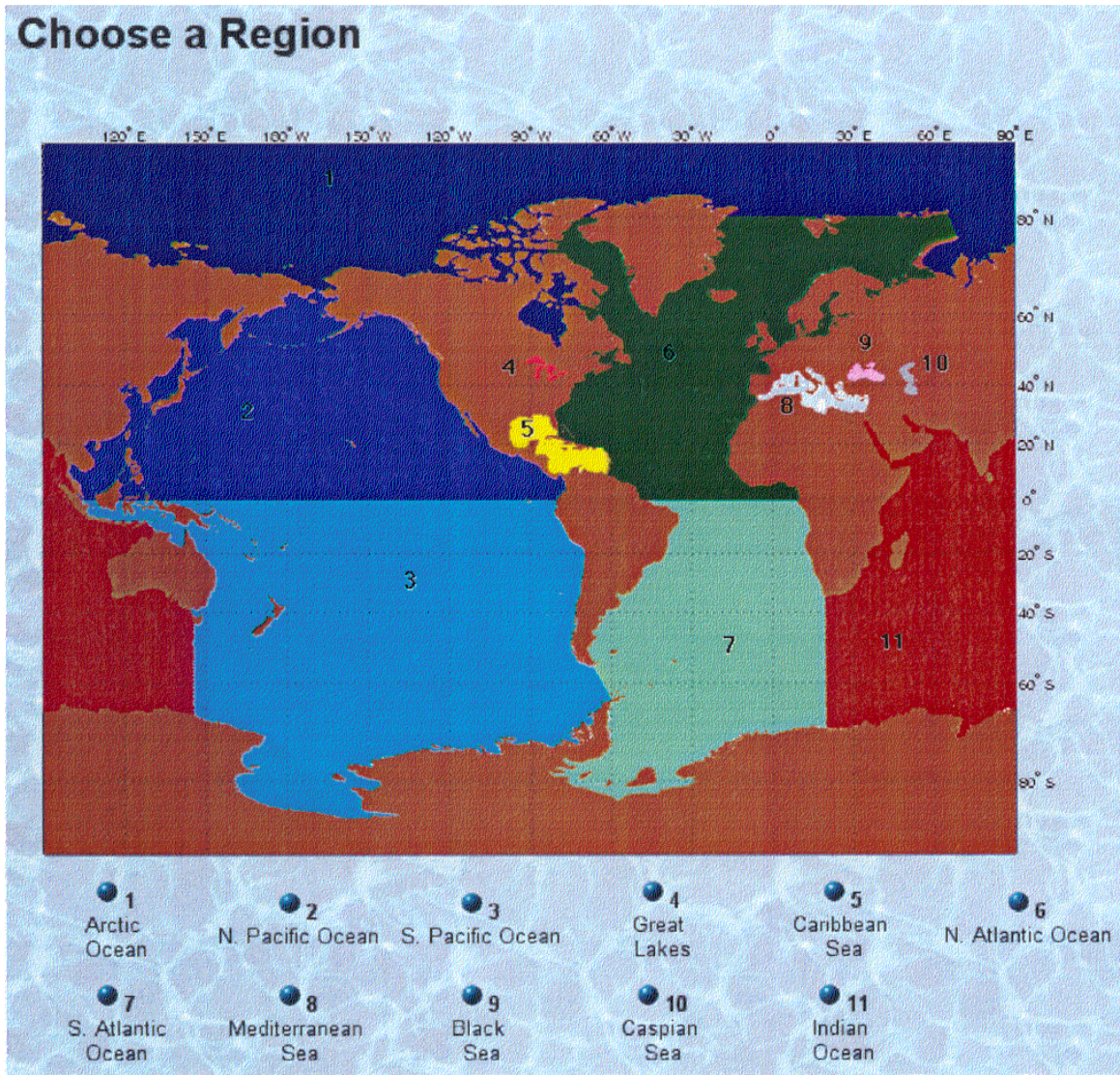


Figure 11 'Search by Ocean Basin' screen of the M-AERI database GUI.

B.1.10.3 Search by Year/Cruise/Month.

The user starts this search selecting a year, cruise, or month from the imagemap, list, or timeline (See Figure 12), and then selects a dataname from the resulting list.

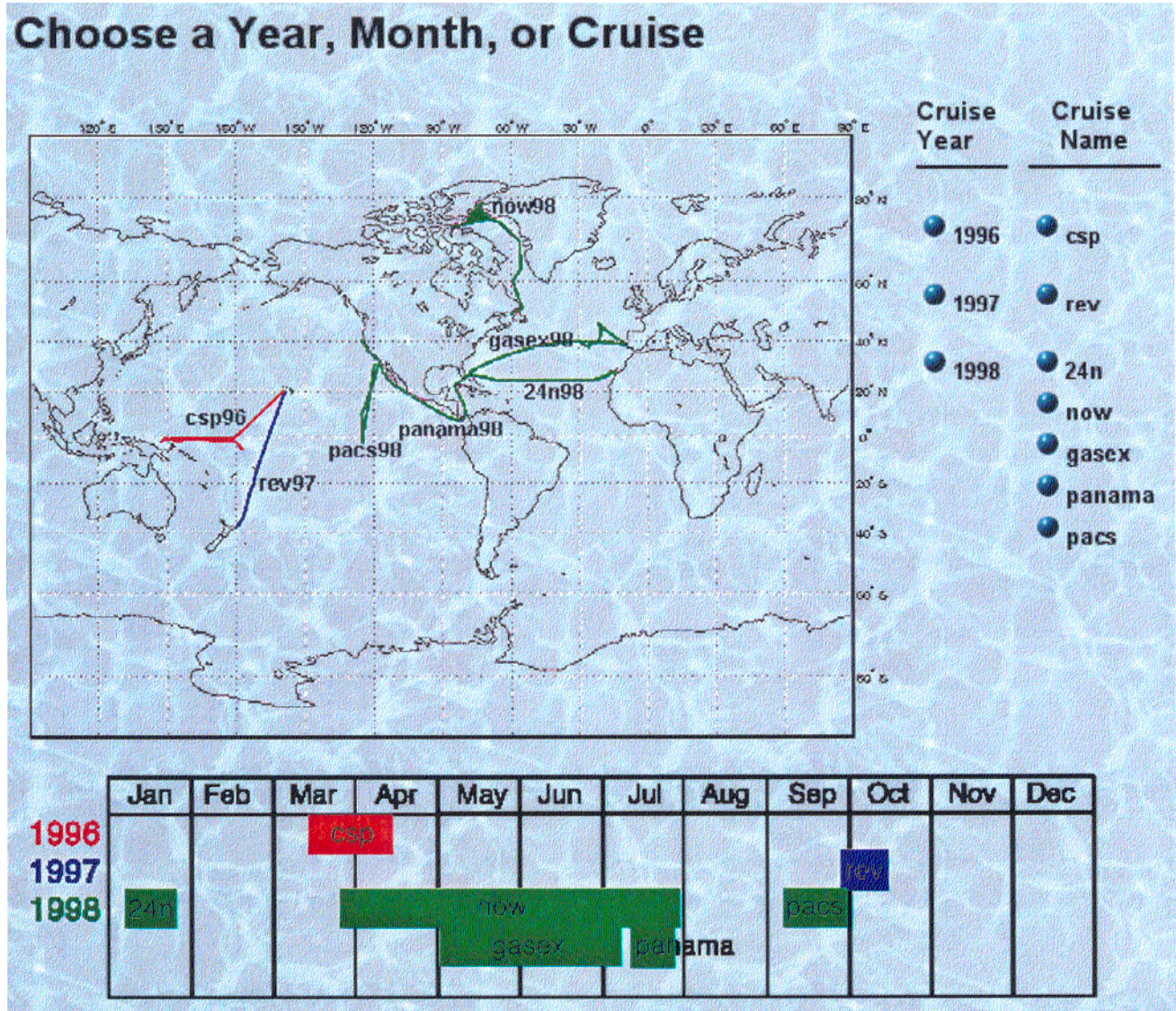


Figure 12. 'Search by Year, Cruise, or Month' of the M-AERI database GUI.

B.1.10.5 Search by SQL Query

This search is for the user who has some knowledge of SQL language and gives them the freedom to type their own query into the text field. The only restrictions are creating, dropping, deleting, or inserting data and/or tables.

B.1.10.6 Search by Matchups

This search is used to find spatial and temporal ‘matchups’ between data sets (or datanames). The page (see Figure 12) is separated into three areas to find matchups between 2D and 2D data, 2D and 3D data, and 3D and 3D data. The 3D by 3D search is going to produce the most output and the user will want to have some idea about the resolution of the data before starting such a large search. The user selects a dataname from the first column, a time interval, a spatial interval, and a dataname from the fourth column. The resultant table consists of side by side matchups of the two data sets.

Matchups

Select an item from each field:

DataName 1, Time Interval, Spatial Interval, DataName 2

2D Data by 2D Data:

MaeriSst HatSst Met	01 sec 05 sec 10 sec 20 sec 30 sec	02 km 04 km 06 km 08 km 10 km	MaeriSst HatSst Met
---------------------------	--	---	---------------------------

Find Matchups

2D Data by 3D Data:

MaeriSst HatSst Met	10 min 15 min 20 min 25 min 30 min	02 km 04 km 06 km 08 km 10 km	MaeriRadSpectra MaeriRadSpectraStats MaeriRet Rsonde
---------------------------	--	---	---

Find Matchups

3D Data by 3D Data:

MaeriRadSpectra MaeriRadSpectraStats MaeriRet Rsonde	50 min 55 min 01 hr 02 hr 03 hr	02 km 04 km 06 km 08 km 10 km	MaeriRadSpectra MaeriRadSpectraStats MaeriRet Rsonde
---	---	---	---

Find Matchups

Figure 12. ‘Search by Matchups’ of the M-AERI database GUI.

B.1.10.7 Search by DataName

This search allows the user to view not only the data tables but also the index tables, which are related to the data tables by key fields. The search starts by selecting a dataname. The next page displays each field in that table and allows the user to search by a particular field value and to pick which fields they would like displayed in the output (Figure 13).

Search by DataName

To search for matching records, enter the values to match against in the text field.
Select which fields to return by checking the boxes to the left of the variable names.
REMEMBER: Use single or double quotes for character strings.

<input checked="" type="checkbox"/>	YYYYMMDD	like	'199603%'
<input checked="" type="checkbox"/>	HHMMSS	=	
<input checked="" type="checkbox"/>	Sec1981	=	
<input checked="" type="checkbox"/>	DecHour	=	
<input checked="" type="checkbox"/>	Lon	=	
<input checked="" type="checkbox"/>	Lat	>=	0
<input type="checkbox"/>	Flag	=	
<input type="checkbox"/>	BasinCode	=	
<input checked="" type="checkbox"/>	IdDay	=	
<input checked="" type="checkbox"/>	IdData	=	
<input checked="" type="checkbox"/>	IdName	=	
<input checked="" type="checkbox"/>	IdProj	=	
<input checked="" type="checkbox"/>	IdInst	=	
<input checked="" type="checkbox"/>	AirTemp	=	
<input checked="" type="checkbox"/>	StdAirTemp	=	
<input checked="" type="checkbox"/>	UncAirTemp	=	
<input checked="" type="checkbox"/>	SkinTemp	=	
<input checked="" type="checkbox"/>	StdSkinTemp	=	
<input checked="" type="checkbox"/>	UncSkinTemp	=	

Choose an output format:
 Table Ascii

To save output as a view, type a view name below:

Figure 13. Fields from the MaeriSst Data Set. the M-AERI database GUI.

This particular search will produce output for all data in March 1996 with latitude values greater than zero degrees and will not display the Flag or BasinCode fields in the output table.

B.1.10.8 Search by DataIndex

This is a search of the tables IndexDaily and IndexData. The user can search by date, longitude, dataname, instrument name, and/or project name, and order the results accordingly (see figure 14).

Search by DataIndex

Enter Date Range in YYYYMMDD Format:

Start Date End Date

Enter Longitude/Latitude Range in Degrees:

Minimum Longitude Maximum Longitude

Minimum Latitude Maximum Latitude

Select One or More Fields : the % sign selects all the options in that field

DataName: InstrumentName: ProjectName:

MaeriRadSpectra
 MaeriRadSpectraStats
 MaeriSst
 HatSst
 Rsonde
 Met
 Ctd

maeri00
 maeri01
 maeri02
 maeri03
 tsg
 wpac
 rawindsonde

pelican95
 csp96
 rev97
 24n98
 now98
 gasex98
 panama98

Order By: Sec1981 Lon Lat DataName InstrumentName ProjectName

Figure 14 Search by 'Dataindex'

This search will produce MaeriSst output from March 3, 1996 to April 15, 1996, for longitude between 20 and 60 degrees east and latitude between 0 and 30 degrees north, for M-AERI instrument number one, and for all projects.

B.1.10.9 Future Work

This database is an evolving structure that will be updated as new data come in from M-AERI projects and matchups are generated with the satellite data. The next step will be to add a graphics interface that will allow the user to make plots of selected data. The database will soon be set up to accommodate MODIS data.

B.1.11. SST data assimilation.

Work has begun to depict the three-dimensional ocean state in near-real time using state-of-the-art ocean models and data assimilation techniques. One of the goals of the collaborative work with Dr. Remy Baraille is to assess the efficiency of a new data assimilation technique, the Adaptive Filter. The Adaptive Filter can also be a very efficient tool to determine the unknown coefficients that are needed (and usually empirically chosen) in classical data assimilation schemes such as Optimal Interpolation, Variational Methods, or Kalman-like filters. The algorithm recursively builds an estimate of the unknown parameters at each data assimilation step by minimizing the forecast errors under some non-demanding hypothesis on model and observation errors (white noise, uncorrelated in time). The estimation process requires the use of the adjoint of the linearized version of the ocean model (the Miami Isopycnic Ocean Coordinate Ocean Model). During the first six months, all the routines needed for the filter (parallelization of the tangent linear, the adjoint, I/Os, ...) were implemented. We are in the process of evaluating the technique with a 1/3 degree North Atlantic configuration which will be compared to Optimal Interpolation schemes using either pre-defined vertical mode sets (Cooper and Haines potential vorticity conservation modes) or vertical correlation coefficients deduced from data.

B.1.12. Refinement of the M-AERI.

Refinement of the M-AERI has focussed on software improvements, including easier operator control over the 'safing' of the scene mirror, and for positioning the mirror for cleaning. Other improvements include a more robust routine for the derivation of skin SST measurements, and a better procedure for laboratory calibration.

B.1.13. Collaboration with the Nansen Centre, Bergen, Norway.

Dr Brian Ward of the Nansen Environmental and Remote Sensing Center is working on the development of a new autonomous profiler, which will carry micro-thermometer capable of measuring the ocean thermal gradients. He has expressed interest in conducting joint experiments with the M-AERI. These are likely to take place later this year.

B.1.14. M-AERI calibration facility

RSMAS took delivery from Hart Scientific Inc. of the water-bath blackbody calibration target, built to NIST design. After brief acceptance tests the calibration target was sent to NIST for certification. On its return to RSMAS it will form the basis of maintaining the accuracy of the M-AERI radiometry and traceability of the derived temperatures to NIST standards.

B.1.15 Wide Area Networking

DS3 circuit to vBNS via FloridaNet continues in operation. This circuit is in the process of being switched over to a University of Miami WAN connection to FloridaNet and should be completed by the next contract reporting period. We are currently Test and characterization of the vBNS link to NASA/GSFC is continuing using new SPRINT connections to GSFC via Chicago. Average available bandwidth is approaching 10Mbs, which is approximately what is needed. We will continue these test and characterization efforts as NASA, SPRINT, vBNS and Abilene improve their peering arrangements. We are hopeful that the currently available bandwidth will be sustained and useable for post-launch data exchange.

C. Investigator Support

January	W. Baringer O. Brown M. Framinan R. Jones	K. Kilpatrick R. Kolaczynski R. Kovach A. Mariano	M. Szczodrak J. Splain S. Walsh
February	W. Baringer J. Brown O. Brown M. Framinan R. Jones	K. Kilpatrick R. Kolaczynski R. Kovach A. Li A. Mariano	J. Splain M. Szczodrak S. Walsh
March	R. Baraille W. Baringer J. Brown O. Brown M. Framinan R. Jones	K. Kilpatrick R. Kolaczynski R. Kovach A. Li K. Maillet A. Mariano	P. Minnett R. Sikorski J. Splain M. Szczodrak S. Walsh
April	R. Baraille W. Baringer J. Brown O. Brown M. Framinan R. Jones	R. Kilpatrick R. Kolaczynski R. Kovach A. Li K. Maillet A. Mariano	P. Minnett R. Sikorski J. Splain M. Szczodrak S. Walsh
May	R. Baraille W. Baringer J. Brown	R. Kolaczynski K. Kilpatrick R. Kovach	A. Mariano R. Sikorski J. Splain

O. Brown
M. Framinan

A. Li
K. Maillet

M. Szczodrak
S. Walsh

D. Future Activities

D.1 Algorithms

- a. Continue to develop and test algorithms on global retrievals
- b. Evaluation of global data assimilation statistics for SST fields
- c. Participate in research cruises
- d. Analyze data taken at radiometer and validation workshops
- e. Continue radiative transfer modeling
- f. Continue analysis of research cruise data
- g. Continue to study near-surface temperature gradients
- h. Continue planning of post-launch validation campaigns
- i. Validation Plan updates (as needed)
- j. EOS Science Plan updates (as needed)
- k. Define and implement an extended ATM based network test bed
- l. Continued integration of new workstations into algorithm development environment
- m. Continued participation in MODIS Team activities and calibration working group

D.2 Investigator support

Continue current efforts.

E. Problems

The recent revelations about unexplained degradation in the performance of the FM-1 MODIS, as revealed in the pre-launch thermal-vacuum testing and other characterization measurements, is a very disturbing development. At present it seems difficult, if not impossible, to say whether these are an indication of instrument degradation which could severely compromise the in-flight performance of the instrument and corruption of the data. Failure to reconcile the observed loss of performance with a physical cause leaves a question mark over the scientific integrity of the mission. As with the decision not to recalibrate the PFM MODIS, this has ramifications on the scientific applications of data, which is a loss to the community as a whole. From the point of view of this specific project, these unresolved issues reduce the post-launch validation campaign to an experimental determination of the SST accuracy in a temporally and geographically constrained fashion, rather than an attempt to increase our understanding of the atmospheric and oceanic processes that impose the limits on satellite remote sensing.

F. Publications and Presentations

F.1 Invited presentations :

Minnett, P.J. Applications of infrared hyperspectral measurements made from ships. Institute of Atmospheric Physics, Rome, Italy, June 1999.

Minnett, P.J., J. Hanafin and E. Kearns. Infrared interferometric measurements of the ocean thermal skin temperature. IEEE International Geosciences and Remote Sensing Symposium. Hamburg, Germany. June, 1999.

F.2 Contributed presentations:

Minnett, P.J. Validation of satellite-derived ocean skin temperatures using the M-AERI. Along-Track Scanning Radiometer Workshop. European Space Research Institute, Frascati, Italy. June 1999.

Sikorski, R.J and P.J. Minnett. Skin SST and Air Temperature Measurements Using a Spectral IR Interferometer (M-AERI). Spring 1999 Meeting of the AGU. Boston, MA. June 1999.